Colloid Polym Sci (2008) 286:31–46
DOI 10.1007/s00396-007-1680-2

ORIGINAL CONTRIBUTION

Liquid crystal and solution phases of sodium dodecyl-*p*-benzene sulphonate (NaLAS) and octa-oxyethylene glycol hexadecyl ether ($C_{16}E_8$): 1:1 mixtures in water

Claire Richards · Gordon J. T. Tiddy · Siobhan Casey

Received: 9 February 2007 / Accepted: 25 March 2007 / Published online: 15 May 2007

Abstract The liquid crystals and other phases formed when the mixed surfactant system sodium dodecyl-*p*-benzene sulphonate (NaLAS) and octa-oxyethylene glycol hexadecyl ether ($C_{16}E_8$, 1:1 by weight) is dispersed in water have been investigated using optical microscopy, X-ray diffraction and differential scanning calorimetry. Despite the fact that neat LAS is a multi-phase solid and $C_{16}E_8$ is a crystalline solid, when the two are mixed at temperatures above the melting temperature of the $C_{16}E_8$ with no water present, what appears to be a metastable gel phase formed containing only a small volume fraction of un-dissolved LAS (ca. 5%). Moreover, when water is added to the system, the phase behaviour of the mixture considerably differs to that of either of the individual components. We report a detailed phase study on this mixture here particularly focussing on the 'neat' mixture. The phase behaviour when water is added is also discussed. Particularly interesting is the presence of a micellar phase between the hexagonal and lamellar phases thought to be due to weak interactions between micelles during the transition from rods to discs. In addition, the presence of a low temperature intermediate phase is discussed.

Keywords Surfactant · Liquid crystal · Dissolution · Mixed anionic non-ionic

C. Richards · G. J. T. Tiddy (✉)
School of Chemical Engineering & Analytical Science,
University of Manchester,
PO Box 88, Manchester M60 1QD, UK
e-mail: Gordon.Tiddy@manchester.ac.uk

S. Casey
Unilever Research Port Sunlight Laboratory,
Quarry Road East, Bebington, Wirral,
Merseyside CH63 3JW, UK

Introduction

Alkylbenzene sulphonates (ABSs) are the most widely used synthetic surfactants, occurring in a range of products from detergents to pesticides. Some decades ago they commonly contained branched hydrocarbon chains, but environmental concerns have resulted in a switch to linear alkyl chain derivatives (LAS). Remarkably, their behaviour has received far less attention than that of much less common surfactants such as sodium dodecyl sulphate. One reason for this is that commercial ABSs contain a distribution of isomers, where the benzene sulphonate group occurs at different locations along the hydrocarbon chain (mid-chain substitution). Secondly, it is difficult to obtain pure compounds because the mid-chain substitution leads to low melting temperatures. The neat surfactants often exist as liquid crystals where impurities are highly soluble, rather than crystals where they are not. Hence, it is difficult to separate the pure surfactant from starting materials in chemical reactions. Nevertheless, one study on a pure isomer shows remarkable behaviour where an upper consolute loop occurs within a lamellar phase [1]. It suggests that a strong attractive interaction occurs between the highly charged bilayers, rather than the expected strong repulsion. This could have important consequences for dissolution rates if it is also present in the commercial mixtures. Because of the unusual behaviour and the importance of ABSs in industry, we have undertaken a more extensive examination of ABS phases generally. This includes the commercial surfactants, purified commercial surfactants (where inorganic electrolyte and organic impurities have been removed) as well as the behaviour of mixtures with other surfactants.

We have current investigations on several commercial dodecyl-*p*-benzene sulphonate systems. To date, we have

reported on unusual multiple-mesophase co-existence for the lamellar phase (L_α)/micellar solution L_1) region of sodium dodecyl-*p*-benzene sulphonate (NaLAS) with water [2]. In this study, we observed multiple X-ray diffraction lines above ca. 40 °C that indicated the existence of multiple lamellar phases. We have also examined the phases formed when a commercial dodecyl-*p*-benzene sulphonic acid is "dry" neutralised with sodium carbonate [3]. Again, several layer phases co-exist, in this case probably due to the formation of mixed acid/salt solids. For mixtures of NaLAS with other surfactants we have examined the behaviour of both anionic and non-ionic second surfactants in a 1:1 (by weight) mixture. A recent paper describes the behaviour of the NaLAS/hexa-oxyethylene glycol dodecyl ether ($C_{12}E_6$, 1:1 mixtures by weight) [4]. This paper describes a similar study using the non-ionic surfactant octa-oxyethylene glycol hexadecyl ether ($C_{16}H_{33}(OCH_2CH_2)_8OH$, $C_{16}E_8$). In the following paragraphs we describe why this non-ionic surfactant was selected. This is followed by a review of the known phase behaviour of the two surfactants alone, together with an outline of what would be expected for the mixture. Our experimental results and conclusions form the major part of this work. The techniques employed were optical microscopy, differential scanning calorimetry (DSC) and X-ray diffraction.

We are interested in developing a general description for the phase behaviour of surfactant systems that includes liquid crystal phases. When considering the behaviour of mixed surfactants, there are well-established theories that allow critical micelle concentrations to be estimated, so that only a few measurements are required to know the behaviour of new surfactants [5]. For the phases formed at high concentrations, the situation is much less clear. With the water-continuous mesophases, the "packing constraints" concepts allow an estimate of micelle shapes. These, together with considerations of allowed volume fractions, can give a qualitative phase diagram for both single and mixed surfactants [6–9]. They apply typically to concentrations up to ca. 70–80% surfactant, where the behaviour of the neat surfactant begins to dominate. In this study, the important factors are the Krafft temperature, or more generally, the Krafft boundary [10]. However, there are few systematic studies where these ideas have been tested in real systems. The present results allow the utility of this approach to be judged.

Predictions from packing constraints

From the alkyl chain [6, 7] and micelle volume fraction [8, 9] "packing constraints", concepts one can obtain an overall picture of surfactant phase behaviour. A brief description is given here. We assume that there are three idealised micelle shapes: spheres, rods and discs. Micellar solutions (L_1) exist only up to a certain concentration of surfactant because the micelles become ordered, forming mesophases at higher concentrations. The micelles are assumed to be smooth, with a sharp boundary between the aqueous (head groups plus water) and hydrophobic (all alkyl chains) regions. The radii (r) of spherical and rod micelles cannot be larger than the all-trans alkyl chain (l_t). Hence, as the area of the head group at the micelle surface (a) decreases, the sequence of micelle shapes is sphere → rod → disc. The transitions occur when $a=3v/l_t$ (sphere → rod) and $a=2v/l_t$ (rod → disc, where v=volume of hydrophobic group). With conventional surfactants having a linear alkyl chain the shape transitions occur at a=ca. 68 Å^2 (sphere/rod) and a=ca. 46 Å^2 (rod/disc).

For the liquid crystals, the first mesophase observed usually has micelles of the same shape as the L_1 phase. Thus spheres give a small micelle (I_1) cubic phase, rods give hexagonal phase (H_1) and discs give lamellar phase (L_α). The initial formation of mesophases occurs when no more micelles can be incorporated into the disordered solution (L_1) without an ordered phase forming because of the various repulsive interactions between the micelles. This is represented by L_1:V_{max}. The actual value (the

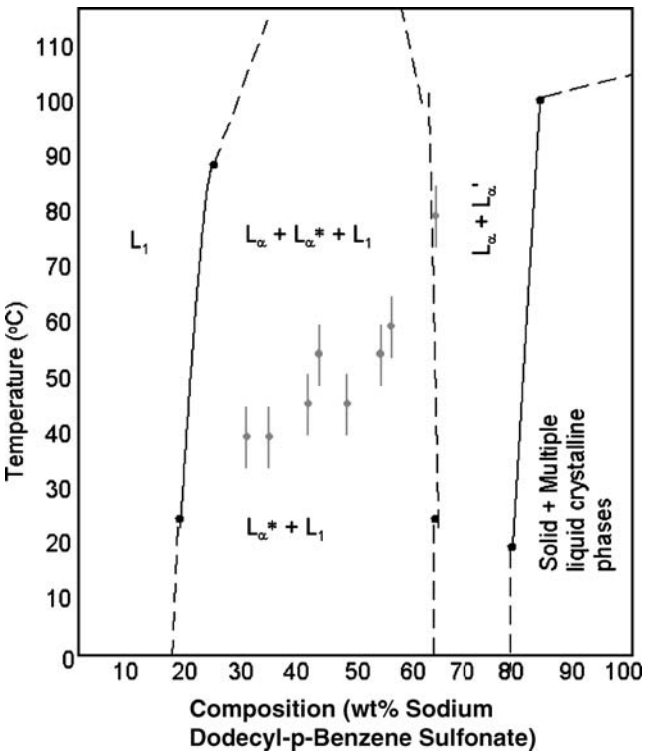

Fig. 1 Phase diagram of the NaLAS/water system. A micellar solution is observed at low concentrations (L_1). Next is a multi-phase region where two or more L_α phases co-exist with a micellar solution. In this region L'_α is used to denote the appearance of two or more L_α phases. L^*_α indicates a situation whereby multiple L_α phases coexist with L_1 above the temperatures indicated by *grey bars* (observed using X-ray diffraction). In the concentrated region, solid and multiple liquid crystalline phases co-exist

Table 1 Alkyl chain and isomer distribution of the sodium dodecyl-*p*-benzene sulfonate (NaLAS)

Isomer	Alkyl chain distribution (wt% of sample)			
	C_{10}	C_{11}	C_{12}	C_{13}
>4-Phenyl	4.2	17.0	18.9	7.5
4-Phenyl	3.2	8.3	5.1	2.0
3-Phenyl	3.1	7.8	4.9	1.8
2-Phenyl	3.2	7.4	4.4	1.2
Total	13.7	40.5	33.2	12.6

Data were taken from [4]

maximum concentration of L_1) decreases as micelle curvature decreases. Thus, L_1:V_{max}:disc micelles < L_1:V_{max}:rod micelles < L_1:V_{max}:spherical micelles. The mesophase sequence with increasing surfactant concentration is determined by the maximum volume fraction (V_{max}) that can be occupied by micelles of a particular shape. It increases as the curvature of the micelles decreases (spheres, V_{max}=ca. 74%; rods, V_{max}=ca. 91%; discs, V_{max}= 100%). Thus, the phase sequence for spherical micelles is: L_1 → small-micelle cubic (I_1) → hexagonal (H_1) → bicontinuous cubic (V_1) [or various intermediate phases (Int)] → lamellar phase (L_α). For rod micelles, the sequence starts at L_1→ hexagonal, and is then the same, whilst for discs it is L_1 → lamellar phase.

The system selected

We have already published some information on the phase behaviour of sodium dodecyl-*p*-benzene sulphonate (NaLAS) with water (Fig. 1) [2]. This material, which has had impurities removed, has the distribution of isomers shown in Table 1. This shows a micellar solution below ca. 20 wt% NaLAS and a large $L_1 + L_\alpha$ region over ca. 20–65%. Beyond this is a region containing multiple lamellar

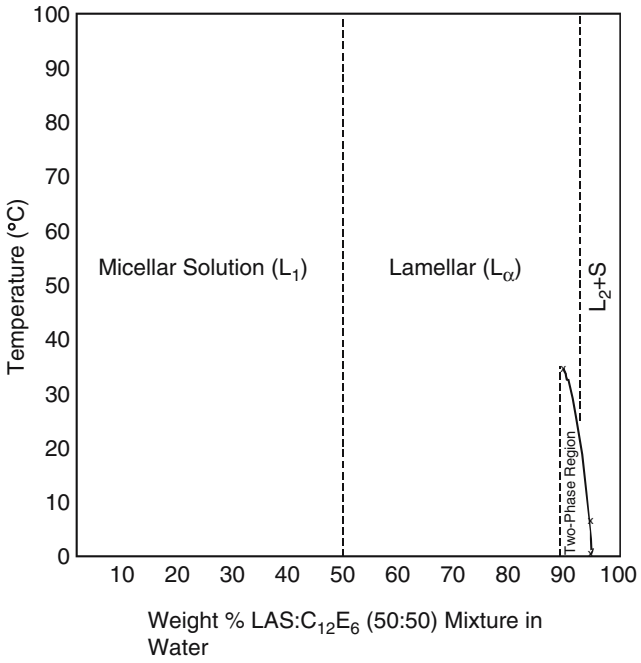

Fig. 3 Phase diagram of NaLAS: $C_{12}E_6$ (50:50)/water system [4]. The "solid" phase "S" at the highest concentrations is probably similar to (some of) the phases present in the NaLAS system. The "two phase region" consists of a lamellar phase with unidentified structures

and more solid-like phases, where the phase structure depends strongly on sample history. Even in the $L_1 + L_\alpha$ region, where only two phases might be expected, we see up to five low angle X-ray reflections above ca. 40–50 °C. These arise from the L_α region, but they differ with composition, so that the system deviates strongly from the Gibbs phase rule. It indicates that several L_α phases are present rather than one. We also have a considerable body of data on the even more complex very high concentration region [11].

We examined the behaviour of NaLAS with hexaoxyethylene glycol dodecyl ether ($C_{12}E_6$, 1:1 mixtures by weight) [4]. This non-ionic surfactant has the phase

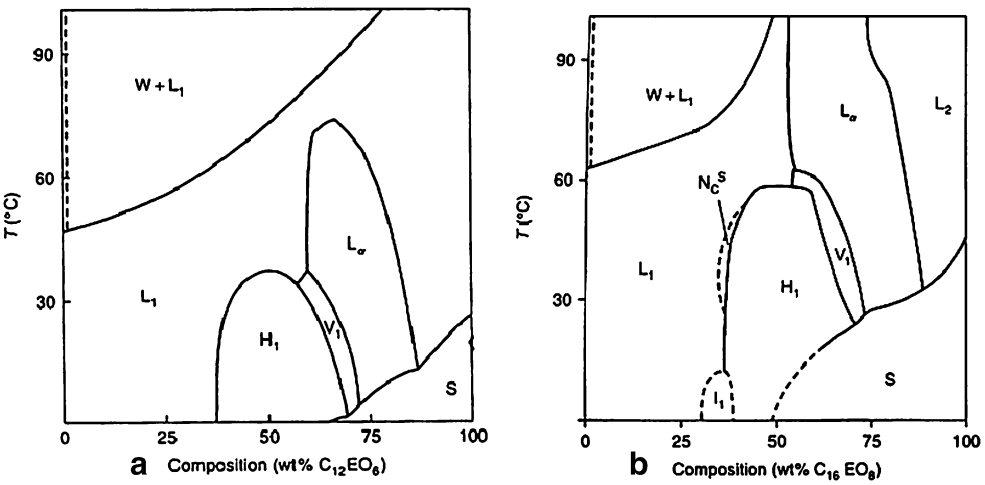

Fig. 2 **a** Phase diagram of the $C_{12}EO_6$/water system from reference [2]; **b** phase diagram of the $C_{16}EO_8$/water system from reference [14]. [The phases are: dilute surfactant solution (W), micellar solution (L_1), rod micelle nematic (N_C), small micelle cubic (I_1), hexagonal (H_1), bicontinuous cubic (V_1) and lamellar (L_α) liquid crystalline phases; solid surfactant is present in area S]

behaviour shown in Fig. 2; it has a relatively low melting point, three liquid crystalline phases and a large solution region. The values of a, v, and l_t are known for the individual surfactants.

To apply micelle packing constraints to mixed surfactants, one requires values of a, v, and l_t for the mixed micelles. Where the chain lengths of the surfactants differ, that of the longest surfactant determines l_t. We assume that a and v are un-altered. Taking the average value of chain volumes and areas, together with an estimated value of l_t for the longest 20% of the surfactants, we calculate that al_t/v=2.3, indicating the formation of H_1, V_1 and L_α phases. The actual phase diagram is given in Fig. 3.

The major regions of the diagram are occupied by micellar and lamellar phases. Thus the real value of al_t/v for the surfactant mixture is ca. 2.0 (if it were smaller, the lamellar phase would form at much lower concentrations). Furthermore, the existence of a liquid non-ionic-rich phase (L_2) at the highest concentrations is unusual since we expect mixing of the surfactant with the NaLAS components that form the neat liquid crystals. Hence, we decided to examine a more "solid-like" non-ionic surfactant with a larger head group in mixtures with NaLAS [octa-oxyethylene glycol hexadecyl ether ($C_{16}H_{33}(OCH_2CH_2)_8OH$, $C_{16}E_8$)]. This surfactant has the phase behaviour shown in Fig. 2 [12]. There is an I_1 cubic phase at low temperatures, so here, the value of al_t/v must be ca. 3, whereas the value falls to ca. 2 at higher temperatures where only a lamellar phase occurs. Whilst no indication of the presence of a gel (layer) phase (L_β) is given in Fig. 2 or the earlier report [8], such a phase does occur with the closely related surfactant hexa-oxyethylene glycol hexadecyl ether ($C_{16}H_{33}(OCH_2CH_2)_6OH$, $C_{16}E_6$) at lower temperatures [13]. The L_β phase has a layer structure similar to L_α, but the alkyl chains are in a rigid "rotator" state [9]. There is a real possibility that this might be stabilised by the longer NaLAS isomers.

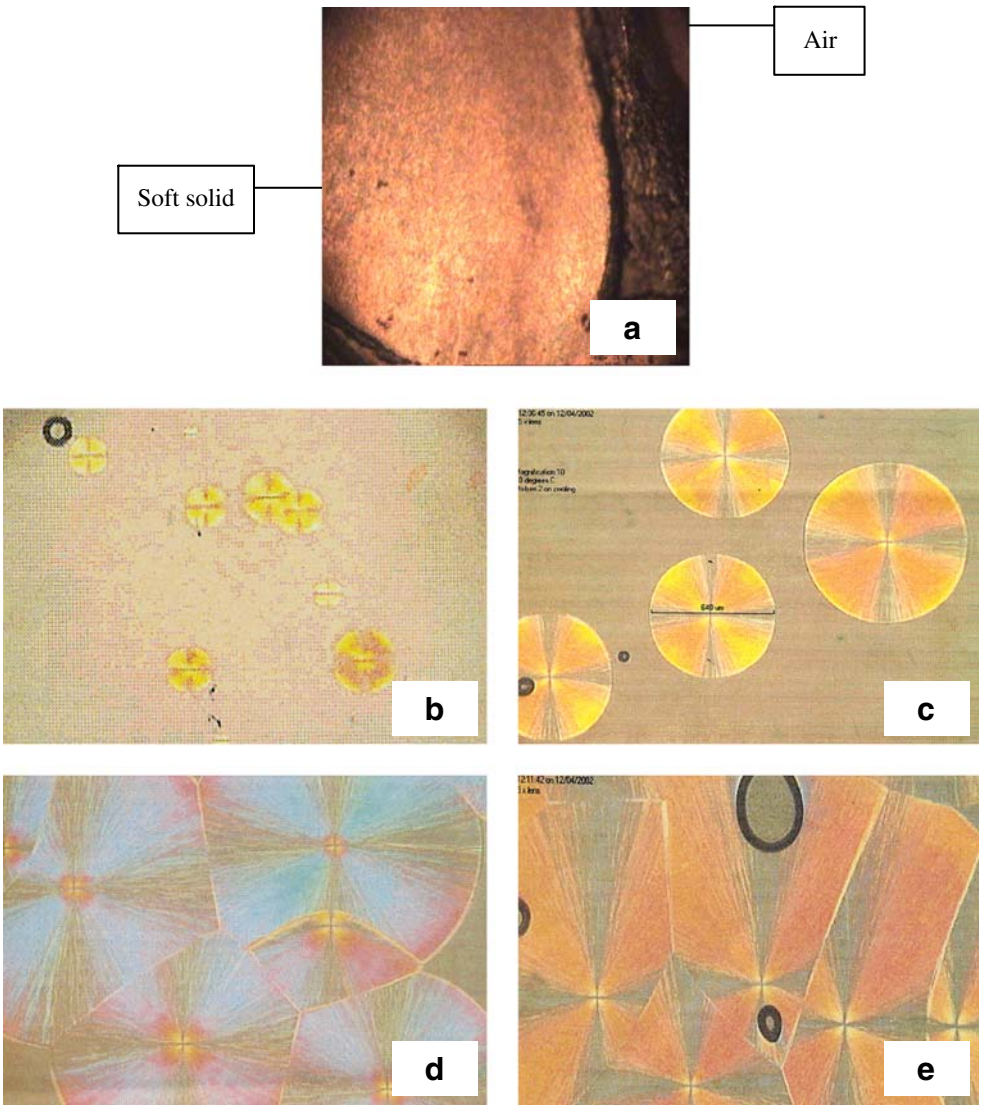

Fig. 4 Optical textures observed on heating 50:50 LAS/$C_{16}E_8$ mixture with no water; **a** birefringence observed for NaLAS/$C_{16}E_8$ in the absence of water. Bulk mixture was heated to 75 °C cooled and left for 3 weeks. (Crossed polarisers, sample width=2.4 mm). **b** Spherulites in isotropic solution appearing after cooling to 10 °C (after approx. 2 min at 10 °C) **c** spherulite growth, **d** further growth, **e** texture of entire sample after a period at 10 °C (approx. 10 min). **a** and **b** partially crossed polarisers, **c** and **d** crossed polarisers. **b**, **c** and **d** 2.4 mm, **e** 1.2 mm

To assess the mesophases expected, we require the value of $\alpha l_t/v$ for the surfactant mixture. The $C_{16}E_8$ used here is a pure, with a straight, un-branched chain. The all-trans chain length (l_t) is 21.35 Å [8] (calculated from known bond-length data [14]), the head group area (a) is 50.5 Å^2 [15], and the volume of the hydrophobic portion (v) is 459 Å^3 (calculated from known density data [14]) then al_t/v=2.35 at 25 °C. The packing parameter for LAS is 2.33 [4]. Since $C_{16}E_8$ has the longest chain length, we must use this as the value for l_t when calculating al_t/v for the mixture. With the averages for a and v, we calculate a packing parameter of 2.63 for the mixture (1:1 by weight). Rod micelles would therefore be expected for this system and a liquid crystalline phase sequence of $H_1 - V_1 - L_\alpha$.

Experimental

The sodium dodecyl-*p*-benzene sulphonate (NaLAS) was a commercial material obtained from Unilever. It had been freeze-dried following the removal of excess sodium sulphate (<0.6% remaining) and organic impurities (<0.1% remaining). The material was stored in a sealed container in a dessicator. A full analysis obtained at Unilever by mass spectroscopy (isomer and chain length distribution) is given in Table 1. $C_{16}EO_8$ was pure material (>99.7% as determined by gas chromatography) obtained from Sigma Aldrich and used as received.

All optical microscopy experiments were carried out using a Carl Zeiss Axioplan-2 polarising optical microscope; photographs were taken using a JVC-TK 1280E CCD camera and analysed using image analysis software attached to the microscope. Where required, temperature control was obtained using a Linkam hot-stage attachment for the optical microscope with an accuracy of ±1 °C. Cooling rates were controlled using a stream of nitrogen gas from a reservoir of liquid nitrogen, thus allowing rapid cooling rates to be obtained.

Small angle X-ray diffraction was carried out on station 16.1 at the Synchrotron Radiation Source (SRS), Daresbury Laboratories, Warrington with X-rays of wavelength 1.4 Å. The detector used was a Quantum 4 ADS. Samples were contained in heat sealed Lindemann tubes to prevent water loss and heating and cooling was carried out using a Linkam hot stage made specifically for capillaries. Temperatures were obtained with an accuracy of ±0.5 °C. Typical heating and cooling rates employed were 10 °C/min with equilibration times of 2 min. Some measurements were also carried out using a laboratory Bruker d8 low-intensity diffractometer.

All DSC measurements were carried out on a thermal analysis DSC Q100. The samples were placed into hermetically sealed aluminium sample pans to prevent water loss. They were weighed before and after the experiment to ensure no water had been lost. The instrument was calibrated using a known amount of indium, which has a very sharp melting temperature of 156.6 °C. All traces were measured at a rate of 5 °C per minute after heat–cool–reheat cycles between the temperatures of 0–100 °C.

For each of the surfactant mixtures, samples were prepared by heating the required amounts of both surfactants with water to 75 °C and centrifuging (both upright and

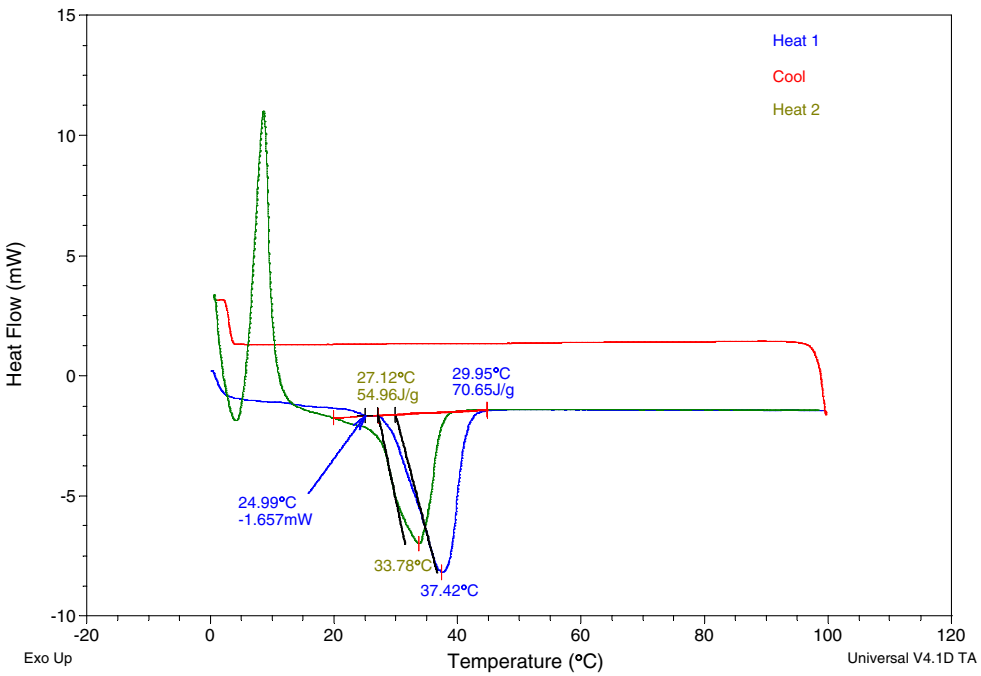

Fig. 5 DSC of NaLAS/$C_{16}E_8$ mixture (no water). Sample heated from 0 to 100 °C at a rate of 5 °C min^{-1} and subsequently cooled to 0 °C and left for 15 min (Bottom two curves are heating scans, top is cooling scan. Peak at 37.4 °C is for first heating scan.)

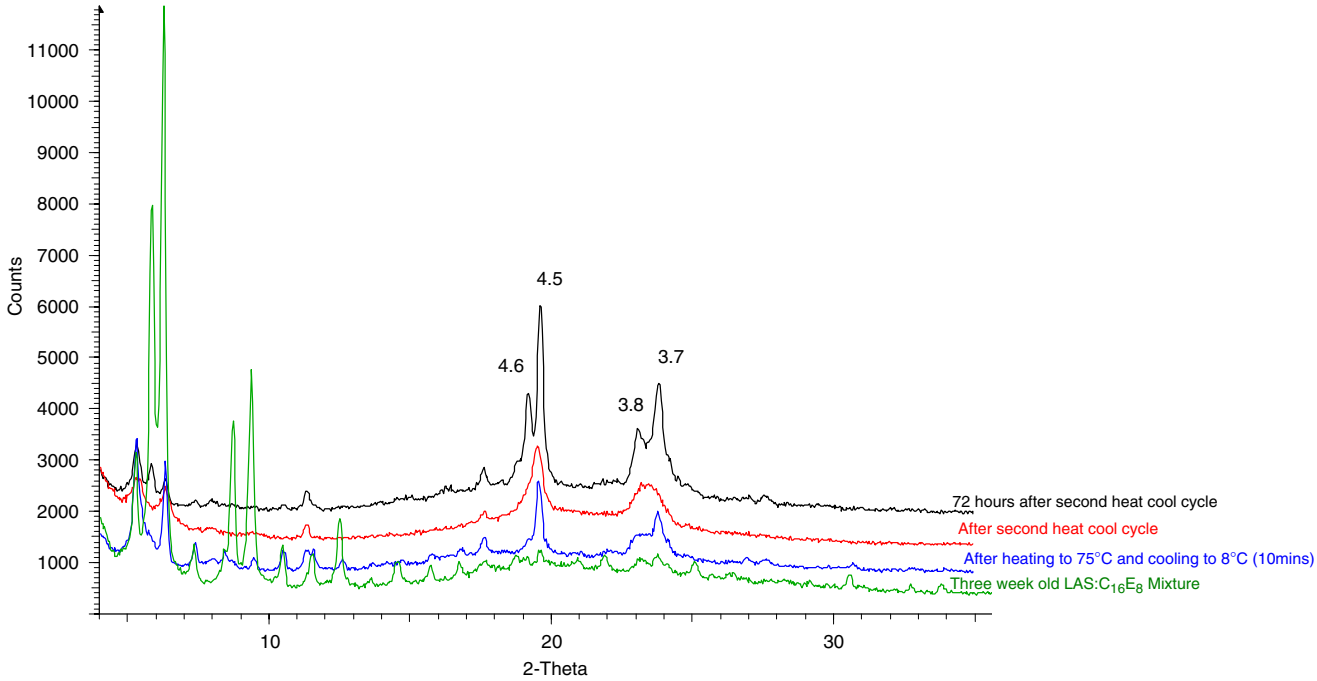

Fig. 6 X-ray data for NaLAS/$C_{16}E_8$ mixture (no water, Bruker diffractometer) at 25 °C (3-week-old material, *green*; 10 min after heating to 75 °C and cooling at 5 °C per minute and down to 8 °C, *blue*; 10 min after a second heat/cool cycle, *red*; 72 h after the second heat/cool cycle, *black*)

inverted tubes) until homogenous (hours to days). Traditionally, the phases of mixed surfactant systems are represented as triangular diagrams, generally at one temperature with each side representing the concentration of surfactant 1, surfactant 2 and of water. To show temperature variance, these are sometimes stacked on top of each other to form a 3D representation. For this work, the weight ratio of surfactant 1: surfactant 2 is always 1:1. The only variables are the amount of water and the temperature. As such, on the phase diagrams presented here each sample studied is

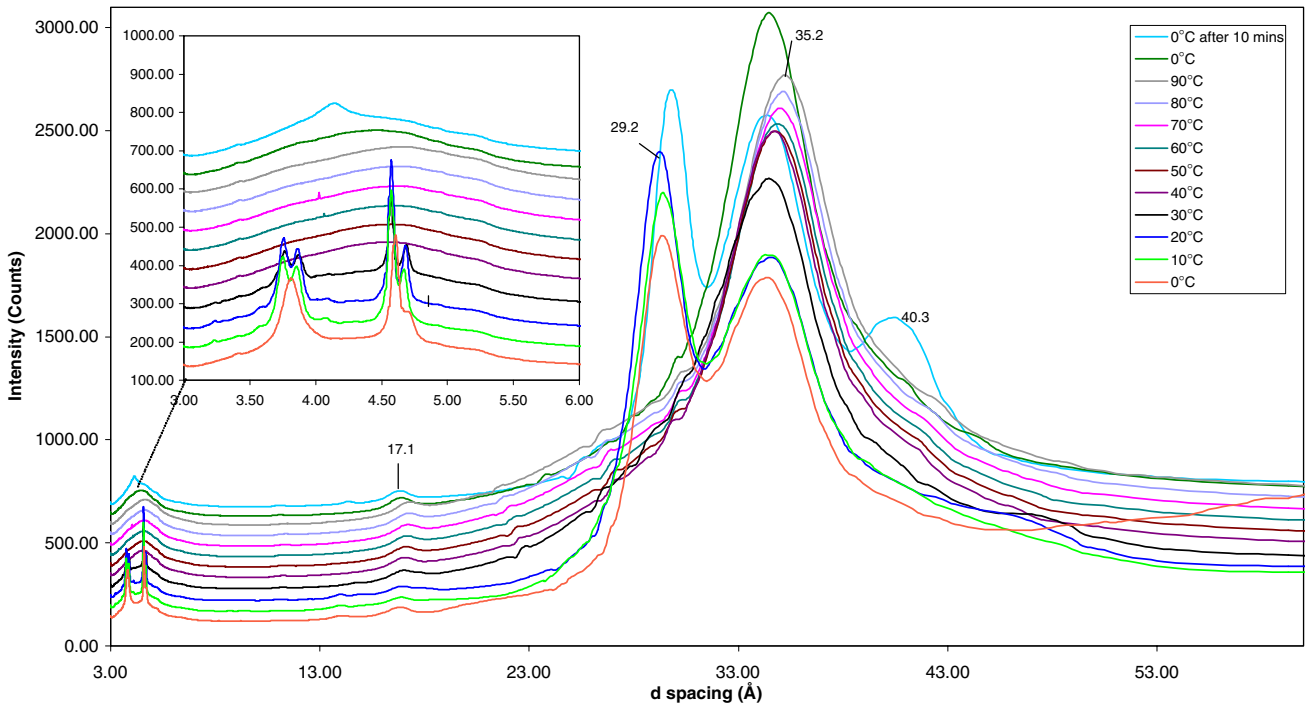

Fig. 7 Variable temperature WAXS data from NaLAS/$C_{16}E_8$ mixture (no water) obtained at SRS Daresbury as a function of temperature. The inset shows wide-angle peaks with spacings of 3.7, 3.8, 4.5 and 4.6 Å. There were however fewer small angle peaks apparent, probably because the sample was only 1-day old. Lowest curve at right hand side is at 0 °C, with curves for 10 °C, 20 °C, ... 90 °C offset above this. The top two curves are for the sample immediately after cooling to 0 °C, and after 10 mins

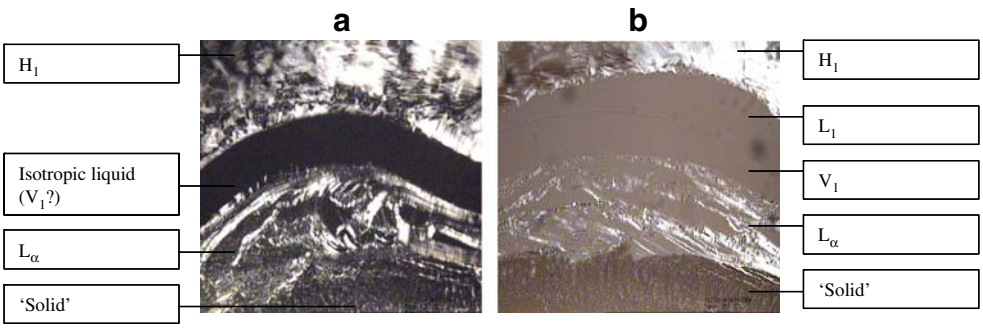

Fig. 8 Optical textures observed during phase penetration scan of NaLAS/$C_{16}E_8$ mixture with water. **a** Phases observed at 25 °C; H_1-Isotropic $(V_1) - L_\alpha$, **b** phases observed at 35 °C; $H_1 - L_1 - V_1 - L_\alpha$. (**a** crossed polars, **b** partially crossed polars, width of each image: 1.2 mm)

represented as % mixture in water. (So for 40% component one, 40% component two and 20% water this would be represented as 80% mixture in water on the phase diagram). Note, however, that some phase compositions of multi-phase samples may not be on the diagram.

Phase behaviour of NaLAS/$C_{16}E_8$ mixture (no water)

A sample of the NaLAS/$C_{16}E_8$ mixture was prepared by heating the two components (4 g total) to 75 °C with agitation until the sample appeared to be homogenous. The sample was cooled to room temperature and stored for at least 3 weeks before the initial experiments were carried out. On reheating to around 50 °C (above the melting temperature of the $C_{16}E_8$−42 °C), the mixture became almost completely an isotropic liquid. There is a small amount of un-dissolved material that persists to high temperatures. It appears to be a minor NaLAS component, possibly with the residual sodium sulphate as well. As was observed with $C_{12}E_6$ mixtures [4], it forms irregular, birefringent, soft crystals not commonly observed for inorganic solids. (See Fig. 2 in [4] for the optical textures). We estimate the volume fraction of this un-dissolved material as ca. 5% or less. However, contrary to the NaLAS/$C_{12}E_6$ mixture, on cooling to room temperature, the liquid persists, but then "solidified" after around 10 min to form a sticky soft 'paste'. This mixture was stored for 3 weeks before a portion was removed and placed under the optical microscope. At this stage, the viscosity had notably increased compared to that observed immediately after heating and cooling. At 25 °C, the substance had no recognisable optical textures yet appeared birefringent under crossed polarisers suggesting that there was some liquid crystalline material present (Fig. 4).

On heating, the mixture melted at 42 °C, seemingly to give an isotropic liquid together with the small fraction of dispersed "solid" (see above). On re-cooling (at a rate of 10 °C/min), solidification of the material and the sample remained a liquid to 8 °C. After around 2 min at 8 °C, small spherical structures began to appear at random intervals in the liquid (Fig. 4b). These grew slowly as more appeared throughout the rest of the sample (Fig. 4c). Eventually, they grew and merged into each other until the whole sample resembled those in Fig. 4d and e. Note the smooth appearance of the air bubbles in Fig. 4e, suggesting that a soft solid rather than a crystal is present. In fact, the cooled mixture can be described as paste-like because it moves slightly on application of light shear to the coverslip.

DSC measurements were carried out on a sample around 1-week old using similar heating and cooling rates as for the optical microscopy (Fig. 5). The melt observed during the optical microscopy experiment is represented by a fairly

Table 2 Phase behaviour observed during temperature controlled phase penetration scan experiment on NaLAS/$C_{16}E_8$ mixture system

Temperature (°C)	Sequence of Phases with Increasing Surfactant Concentration →					
8-35	L_1	H_1	V_1		L_α	Viscous liquid crystalline phase[a]
35-43.6	L_1	H_1	L_1	V_1	L_α	Viscous liquid crystalline phase(s)[a]
43.6-50	L_1	H_1	L_1		L_α	L_2 + some undissolved LAS
50-100	L_1	L_1			L_α	L_2 + some undissolved LAS
100-43	L_1	L_1			L_α	L_2 + some undissolved LAS
43-8	L_1	H_1	L_1		L_α	L_2 + some undissolved LAS

[a] See Phase behaviour of NaLAS/$C_{16}E_8$ mixture (no water).

Table 3 Phases observed by temperature-controlled optical microscopy experiments on heating samples of known composition for the NaLAS/$C_{16}E_8$ mixture in water

Sample Composition (Wt. % LAS:$C_{16}E_8$ (50:50) mixture in water)	Temperature (˚C)										
	3	10	20	30	40	50	60	70	80	90	100
10	L_1										
20	L_1										
30	L_1										
35	Intermediate (Int.)? (15.5˚C)		H_1 (39˚C)			L_1					
40	Int.? (18˚C)			L_1							
45	Int.? (18.5˚C)			L_1							
50	L_1										
52	L_1										
57	L_α (95˚C)										L_1
60	L_α(75.7˚C)								L_1		
70	L_α (93˚C)									L_1	
80	L_α (98˚C)										L_1
85	L_α										
90	L_α + S (15˚C)				L_α						
95	L_α + S (20˚C)				L_α						
100	S (50˚C)						Isotropic liquid + S				

Temperatures in brackets are those at which transitions were observed.

broad transition at 37 °C with a large ΔH value (70.7 J/g). This is about half the value expected for melting of a crystalline solid [16]. There also appears to be a very small transition/pre-transition just before this at around 25 °C, although the ΔH value was too small to measure. No solidification peak was observed on cooling, which was consistent with the optical microscopy experiment although one does appear on the re-heat at ca. 8 °C, thus confirming that there is considerable hysteresis in the heating and cooling cycles. On the second heat cycle, only one endothermic transition is present at a somewhat lower temperature than on the first heating cycle. This suggests

Table 4 Phases observed by temperature-controlled optical microscopy experiments on cooling samples of known composition for the NaLAS/$C_{16}E_8$ mixture in water

Sample Composition (% LAS:$C_{16}E_8$ (50:50) mixture in water)	Temperature (˚C)										
	3	10	20	30	40	50	60	70	80	90	100
10	L_1										
20	L_1										
30	L_1										
35	Int? (15.5˚C)		H_1 (39^0C)			L		1			
40	Int? (18˚C)			L_1							
45	Int? (18.5˚C)			L_1							
50	L_1										
52	L_1										
57	L_α (95˚C)										L_1
60	L_α(75˚C)				L				1		
70	L_α(93˚C)					L					1
80	L_α (95˚C)										L_1
85	L_α										
90	L_α										
95	L_α										
100	L_2+S[a]										

Temperatures in brackets are those at which transitions were observed.

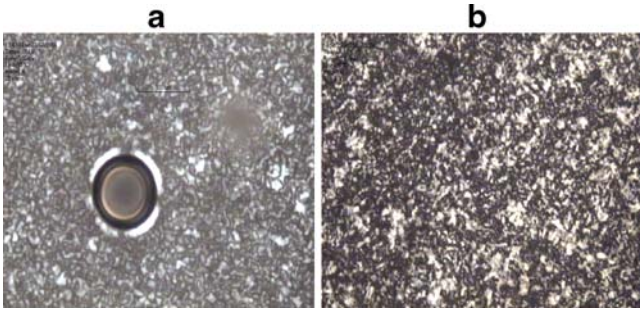

Fig. 9 Optical textures for the intermediate phase; **a** 35% NaLAS/$C_{16}E_8$/65% water at 14.6 °C and **b** 40% NaLAS/$C_{16}E_8$/60% water at 18 °C. (Both crossed polars. Widths **a** 0.6 mm, **b** 1.2 mm)

that after heating and cooling initially, the surfactants mix to form one phase. After 1 week, it appears that there are possibly two phases present suggesting that there may have been some separation of the components. The large enthalpy transition is of the magnitude expected for a gel (L_β) phase, rather than a crystalline solid [9, 16].

X-ray diffraction data for the sample are given in Fig. 6. The initial scan on a 3-week-old sample shows multiple diffraction lines, as expected for a crystalline solid. Note that line intensities may not be a true indication of the powder pattern intensities for scans made on crystalline samples with non-random orientations of the crystals. Most of the lines are very much reduced after the first heat/cool cycle, and only a small number remain after the second cycle. The X-ray data do indeed suggest that after the first two heating and cooling cycles, there is still order in the alkyl chain region (ca. 3.5–4.5 Å). However, the 4.2 Å line observed typically for an L_β phase is not present. Instead, other high angle lines are seen (Fig. 6). The four lines in this region correspond to d spacings of 4.6, 4.5, 3.8 and 3.7 Å. Some of these may indicate an orthorhombic packing of chains [16]. X-ray data taken of the sample 72 h after the heating and cooling cycle suggest that an ordered phase is still present and is therefore fairly long lived. It would be expected, however, that with time, the $C_{16}E_8$ would slowly crystallise, and the substance would contain a mixture of crystalline non-ionic, L_α phase(s) from the LAS and some remaining gel phase.

This experiment was repeated at the Daresbury Synchrotron, on wide-angle station 14.1 (Fig. 7). Non-scientific restrictions meant that the initial sample was only 1-day old. The wide angle peaks with spacings of 3.7, 3.8, 4.5 and 4.6 Å are again seen below ca. 40 °C. There were, however, far fewer small-angle peaks apparent. The peak at ca. 35 Å is present at all temperatures, but the peak at 29.2 Å is present only at low temperatures. A peak at ca. 4.2 Å is present in the sample after the heating/cooling cycle. It is obvious that further measurements are required to fully establish the phase behaviour, but clearly there is a slow re-formation of equilibrium phases after heating, with the presence of gel phases being a strong possibility.

Phase behaviour of NaLAS/$C_{16}E_8$ mixture with water

Optical microscopy

A phase penetration scan experiment [17], where the neat surfactant is contacted with water, was carried out to give a qualitative survey of the mesophases. The surfactant mixture was heated to 80 °C and cooled, before preparation of the microscopy samples. The initial contact with water took place at 8 °C. A hexagonal phase (H_1) phase was first to form followed by bi-continuous cubic phase (V_1) and a lamellar phase (L_α; see Fig. 8a). On heating to 35 °C, the H_1 phase began to melt to form a liquid phase (L_1) as seen in Fig. 8b.

At 39 °C, the H_1 and V_1 phase continued to melt into a liquid phase with the V_1 phase eventually totally melting at 43.6 °C leaving a phase sequence of $H_1 - V_1 - L_\alpha$. On further heating to 50 °C, the H_1 phase melted leaving a phase sequence of $L_1 - L_\alpha - L_2$; recall that at this temperature, the 'solid' mixture had melted. These phases persisted to 100 °C. On cooling, the H_1 phase reappeared at 43 °C. However, the V_1 phase did not reappear.

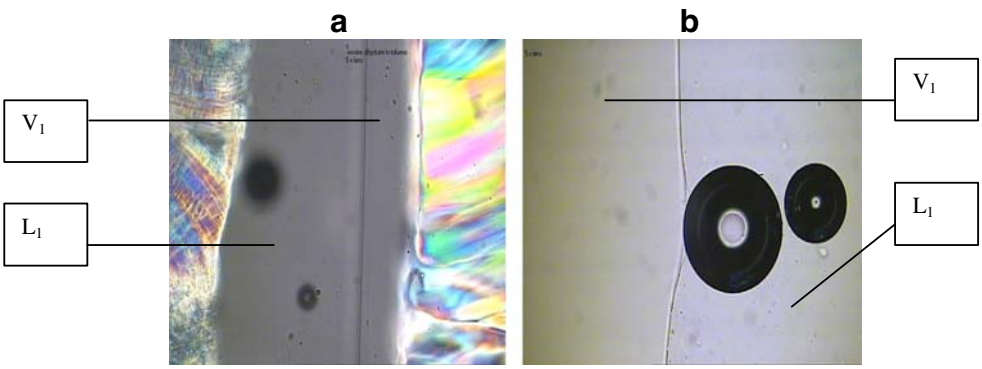

Fig. 10 Optical textures observed during capillary phase penetration scan experiment of NaLAS/$C_{16}E_8$ mixture. **a** Shows the presence of a liquid phase between the L_α and the V_1 phases (partially crossed polarisers, width of image: 2.4 mm), **b** close-up of boundary between V_1 and L_1-round air bubbles indicate low viscosity in the L_1 region (partially crossed polars, width: 1.2 mm)

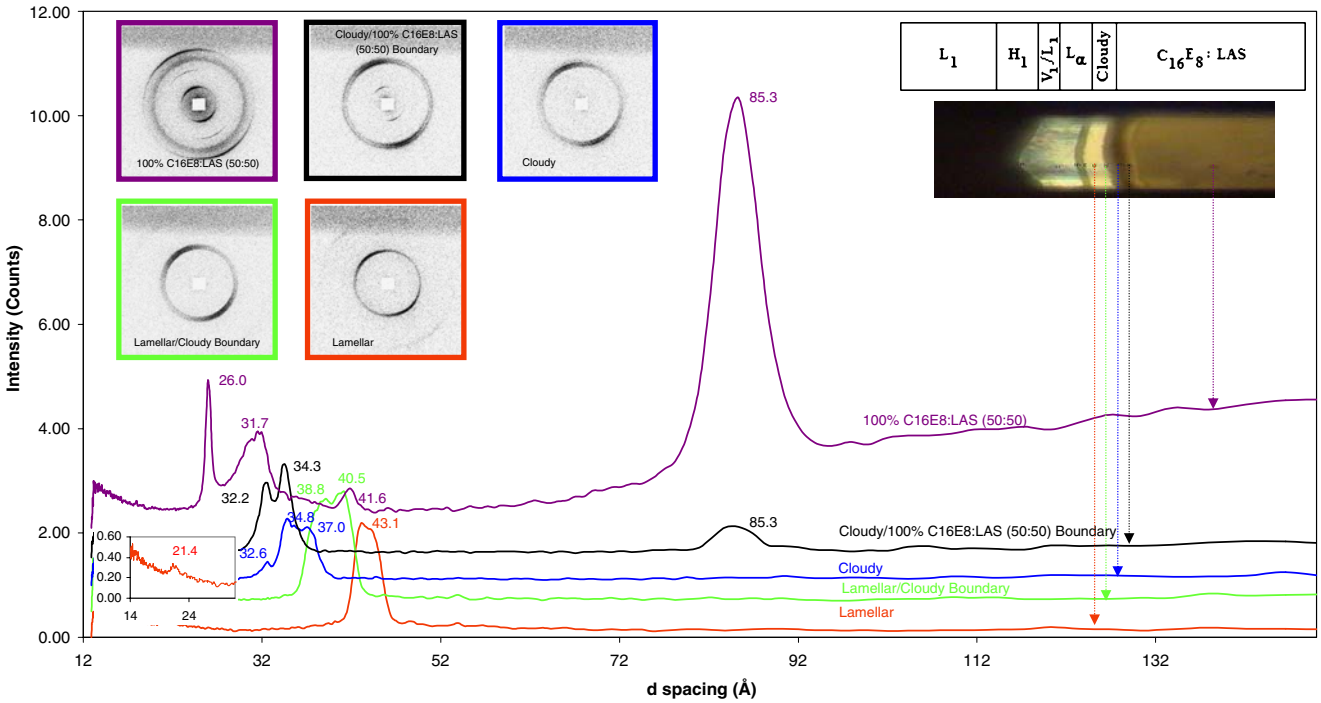

Fig. 11 SAXS data taken at various positions in phase penetration scan of NaLAS/$C_{16}E_8$ with water at room temperature. *Top right hand corner* contains schematic diagram of the phases observed in the capllary and the corresponding photograph taken during the experiment. 2D images are displayed to the *left hand side* with the borders colour coded to each data series. Integrated 1D plots give *d* spacings for each point marked on the photograph

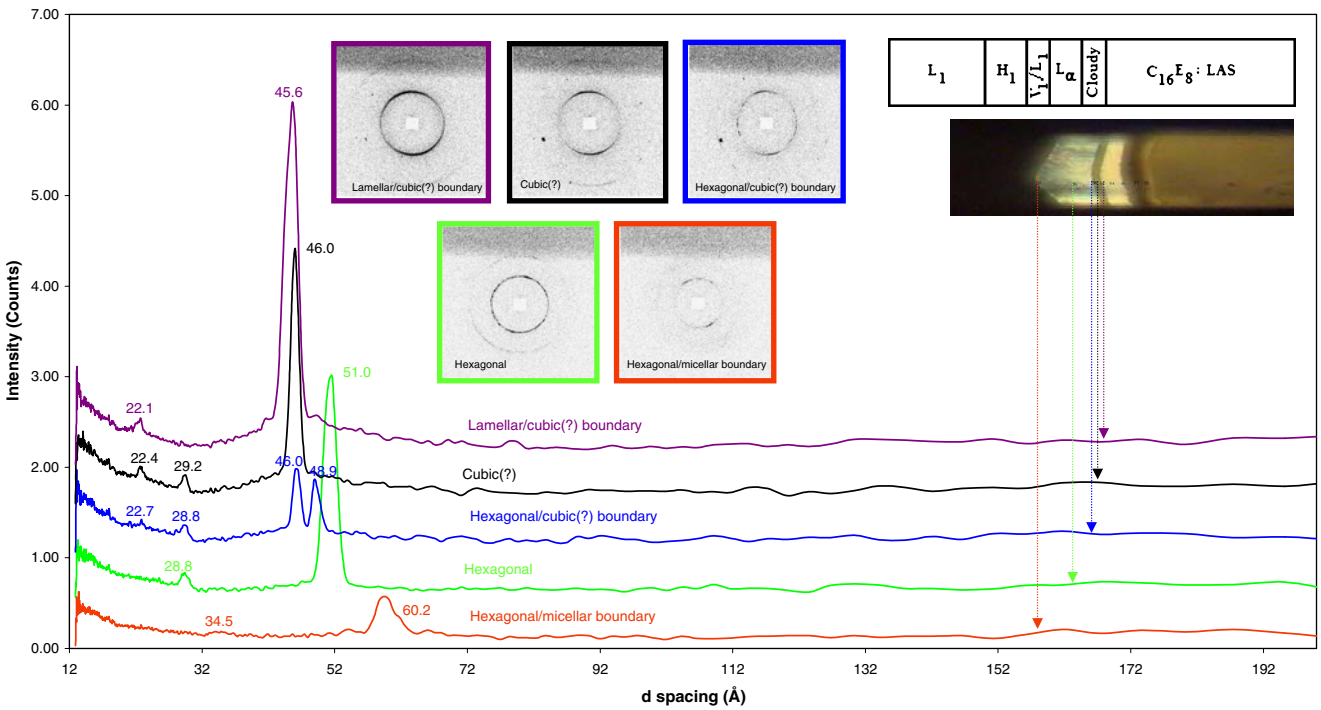

Fig. 12 SAXS data taken at various positions in phase penetration scan of NaLAS/$C_{16}E_8$ with water at room temperature. Further details given above (Fig. 11)

Table 5 *d* Spacings and corresponding microscope observations for samples of known composition NaLAS/$C_{16}E_8$ with water at 25 °C

Sample composition [% LAS/$C_{16}E_8$ (50:50) mixture in water]	d_o (Å)	$d/2$ (Å)	$d/\sqrt{3}$ (Å)	Microscope observations	Phase
89.9	31.7	15.8		Maltese crosses and oily streak textures	L_α
79.9	34.8	17.2		Maltese crosses and oily streak textures	L_α
70.1	35.3	17.6		Maltese crosses and oily streak textures	L_α
60.0	39.8	19.7		Maltese crosses and oily streak textures	L_α
50.0	Broad diffuse rings: 50.0 (d), 25.4 (~d/2)			Non-viscous isotropic liquid	L_1
40.1	Broad diffuse rings: 53.4 (d), 27.3 (~d/2)			Non-viscous isotropic liquid	L_1
37.0[a]	Broad diffuse rings: 60.80 (d), 30.5 (~d/2)			Non-viscous isotropic liquid	L_1
36.0*	53.3 24.9			Birefringent non-geometric textures	H_1
30.0	Broad diffuse ring: 57.3 (d)			Non-viscous isotropic liquid	L_1
20.0	Broad diffuse ring (difficult to tell spacing)			Non-viscous isotropic liquid	L_1
9.9	Broad diffuse ring (difficult to tell spacing)			Non-viscous isotropic liquid	L_1

[a] Samples marked were carried out using wide-angle X-ray scattering (with poor accuracy for large spacings) while the rest were carried out using small angle

The data obtained during the phase penetration scan are tabulated in Table 2.

Following these observations, samples of known composition were examined by optical microscopy. The samples were heated from 3–100 °C using the Linkam hot-stage. The data are tabulated in Tables 3 and 4 for heating and cooling respectively.

The data obtained here provided a somewhat different picture of the phase behaviour. There is an intermediate phase below 20 °C at ca. 35–45 wt% mixture, not seen in the penetration scan. The optical textures were mosaic-like in nature (Fig. 9), whilst the viscosity was fairly low (slightly more than an L_α phase but less than the H_1 phase). This strongly indicates that the phase has a structure similar to the fluid intermediate phase (Fl) observed by Holmes et al. for the non-ionic surfactant $C_{22}EO_6$, which is similar to the lamellar phase. However, in this phase, the lamellae are broken by water filled defects, which exhibit no correlation in position between layers [18]. Furthermore, no V_1 phase was observed for any sample, but this was a very small region in the penetration scan. The H_1 phase is also a very small region (smaller than it initially seemed during the phase penetration scan experiment). To check the width of this region at 25 °C, several other samples were prepared with compositions around 35%. The composition range at 25 °C is estimated to be 32–37% (+/−0.5%). Perhaps most

Table 6 Compositions of surfactant mixture at various regions in capillary scan

Position in capillary experiment	d spacings (Å)	Mass fraction
100% LAS/$C_{16}E_8$ mixture	85.3, 31.7, 26.0	1.0
Cloudy/100% boundary	85.3, 34.3, 32.2	0.86 and 0.95 (2 phase region)
Cloudy region	37.0, 34.8, 32.6	0.69, 0.85, 0.8 (multi-phase region)
Lamellar/cloudy boundary	40.5, 38.8	Between 0.7, 0.74 (unclear)
Lamellar	43.1 (d), 21.4 (d/2)	0.64
Lamellar/isotropic boundary	45.6 (d), 22.1 (d/2)	0.59
Isotropic (cubic)	46.0 (d), 29.2 ($d/\sqrt{2}$), 22.4 (d/2)	0.54
Hexagonal/isotropic boundary	48.8 (d), 46.1 (d'), 28.8 (d/2), 22.7($d/\sqrt{3}$)	0.5
Hexagonal	51.1 (d), 28.8 ($d/\sqrt{3}$)	?
L_1/hexagonal boundary	60.2 (d), 34.5 ($d/\sqrt{3}$)	?

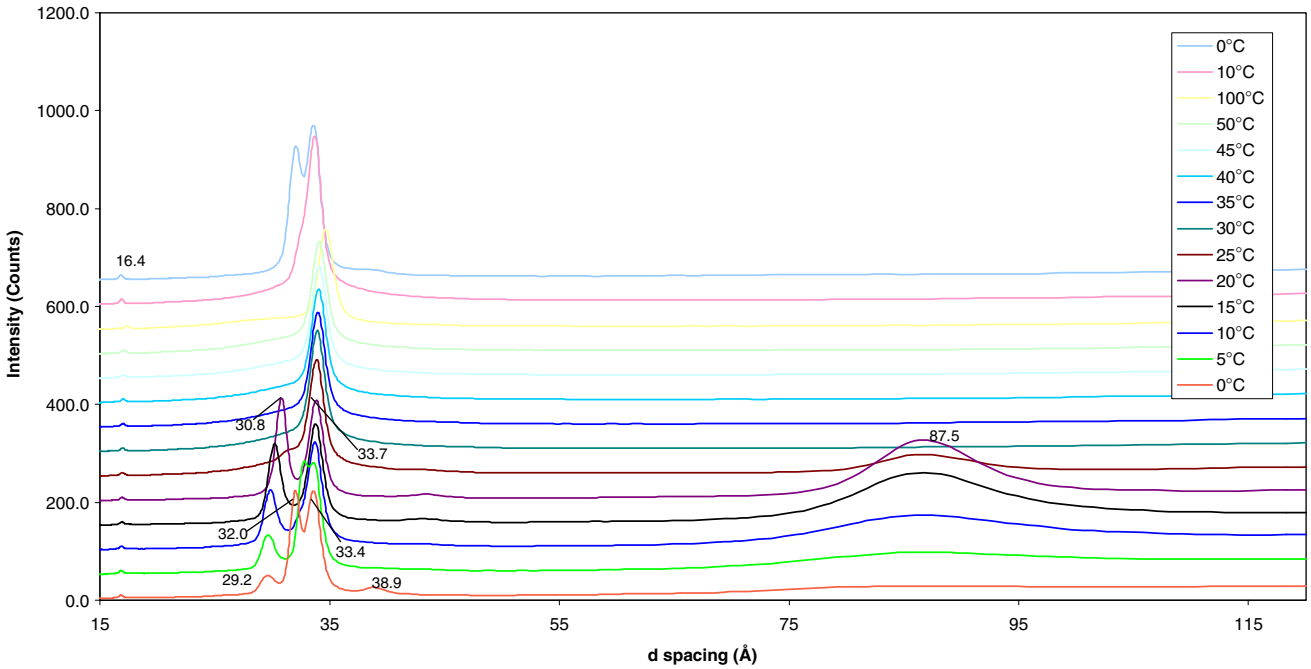

Fig. 13 Variable temperature SAXS study of 95% NaLAS/$C_{16}E_8$ mixture. Shows the presence of a two-phase region below 25 °C that eventually mixes to form a single L_α phase. On cooling, the L_α phase remains to 10 °C where phase separation begins to occur indicated by broadening of peak until at 0 °C two phases become present again. Lowest curve at right hand side is at 0 °C, with curves for 5 °C, 10 °C … 50 °C offset above this. Top 3 curves are for 100 °C, followed by cooling to 10 °C then 0 °C

interesting here is the formation of a large, low viscosity isotropic (micellar) region between the H_1 and L_α phases. This is not seen in binary surfactant/water systems. For further confirmation of the phase structures, we carried out X-ray diffraction measurements.

X-ray diffraction

Small angle X-ray diffraction was firstly used to study a phase penetration scan experiment enclosed in a glass micro-capillary having a rectangular cross-section and a thickness of 1.0 mm. The phases observed agree with those observed during the previous optical microscopy experiments. On contact with water at 25 °C, a cloudy region was initially formed (possibly two-phase). After a couple of minutes, the other mesophases formed became clearer, giving the sequence $L_1 - H_1 - V_1 - L_1 - L_\alpha$–cloudy–100% NaLAS/$C_{16}E_8$ mixture. The optical textures observed confirmed that a liquid phase exists between the H_1 and L_α regions (Fig. 10).

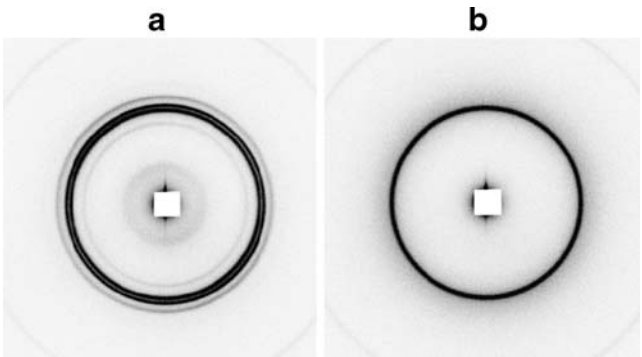

Fig. 14 SAXS 2d images for 95% NaLAS/$C_{16}E_8$ mixture at **a** 0 °C and **b** 30 °C

The X-ray diffraction patterns observed during the capillary controlled phase penetration scan experiment are displayed in Figs. 11 and 12. The isotropic region was studied as one region however since the image quality meant the boundary between the L_1 and the V_1 phase could not be seen. To determine the composition of surfactant at each point in the capillary contained phase penetration scan experiment, a calibration plot was compiled by plotting mass fraction of mixture vs d spacing for a variety of samples of known composition at 25 °C. The data for these samples are tabulated in Table 5.

The d_o spacings listed in Table 5 were subsequently plotted as a function of mass fraction of surfactant mixture. This was then used to estimate compositions at various regions in the phase penetration scan experiment (Table 6).

However, it should be remembered that the phase penetration scan is not at equilibrium, and so the results obtained in this experiment can only be used as a guide to the phase boundary compositions.

To form a better idea of how the phase behaviour changes with temperature, variable temperature X-ray measurements were carried out on a few samples (95% mixture with 5% water, 90% mixture and 36% mixture). Both the 90 and 95% samples were heated to 100 °C at 5 °C

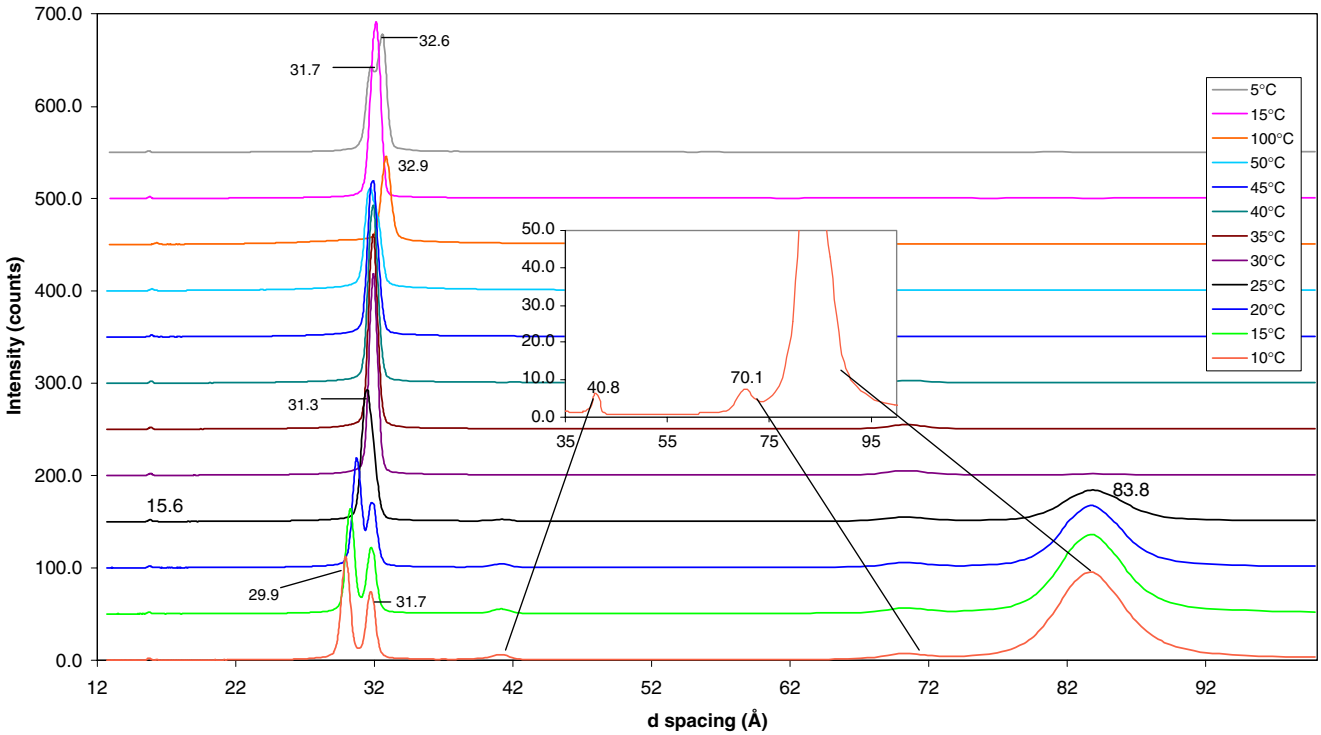

Fig. 15 Variable temperature SAXS study of 90% NaLAS/$C_{16}E_8$ mixture. Lowest curve at right hand side is at 10 °C, with curves for 15 °C, 20 °C … 50 °C offset above this. Top 3 curves are for 100 °C, followed by cooling to 15 °C then 5 °C

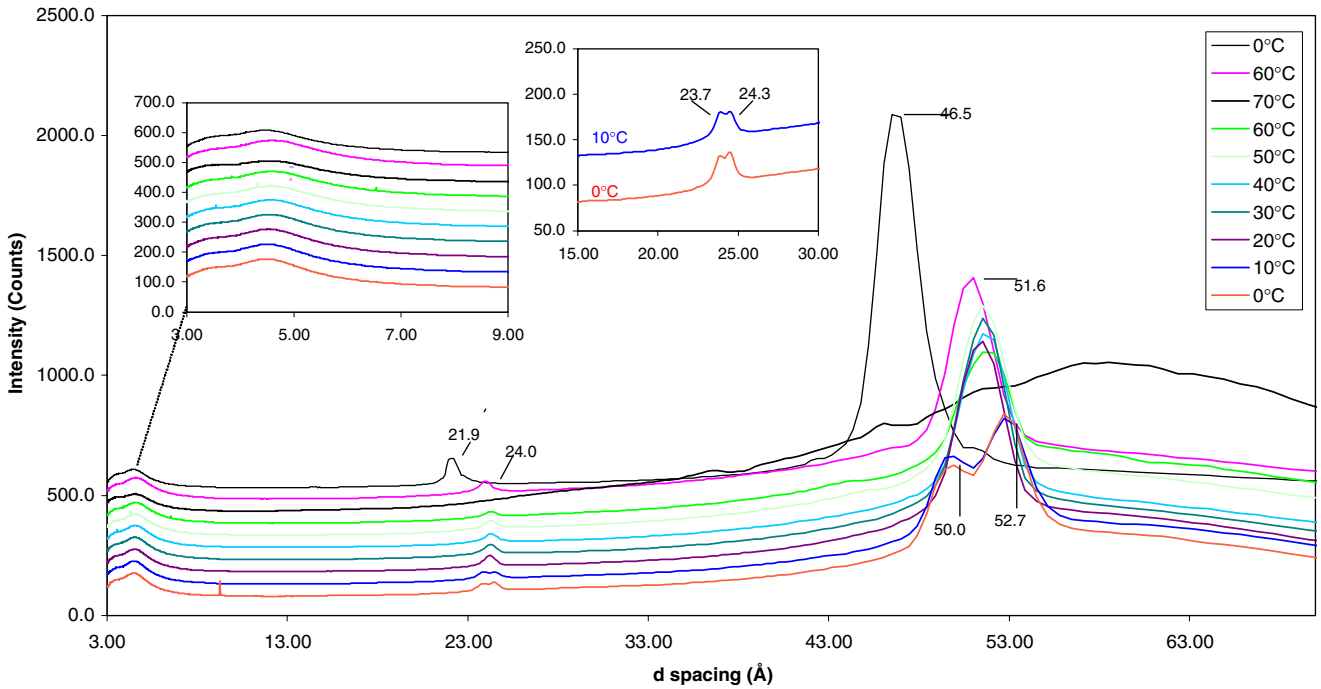

Fig. 16 Variable temperature WAXS study of 36% NaLAS/$C_{16}E_8$ mixture. Inset to main plot are areas of low intensity where zoom has been applied. Lowest curve at right hand side is at 0 °C, with curves for 0 °C, 10 °C … 70 °C offset above this. Top 2 curves are for cooling to 60 °C then 0 °C

Table 7 Transition temperatures and enthalpy changes for DSC on NaLAS/$C_{16}E_8$ samples

Sample composition (wt% LAS/$C_{16}E_8$ in water)	Cycle	No of transitions	Onset temperature (°C)	Peak temperature (°C)	Enthalpy change (J/g)
100%	Heat 1	2	21.2, 27.7	25.4, 33.1	2.4, 22.2
	Cool	0	–	–	–
	Heat 2	2	25.5	28.8	16.2
95%	Heat 1	1	20.7	22.8	27.0
	Cool	1	Exotherm beginning at around 0°C	Not detectable	Not detectable
	Heat 2	1	19.9	23.2	11.0
90%	Heat 1	2	11.6, 27.5	23.3, 30.3	35.1, 0.38
	Cool	0	–	–	–
	Heat 2	1	9.6	21.5	7.58
80%	Heat 1	1	4.12	17.0	2.2
	Cool	0	–	–	–
	Heat 2	0	–	–	–
70%	Heat 1	1	93.0	93.4	0.6
	Cool	1	~100	~95.0	Not measurable
	Heat 2	1	92.7	95.0	0.3
60%	Heat–cool–heat	0	–	–	–
50%	Heat–cool–heat	0	–	–	–
40%	Heat–cool–heat	0	–	–	–
30%	Heat–cool–heat	0	–	–	–

per minute, and a scan was taken every 5 °C. Data for the 95% sample are plotted in Fig. 13.

Data for the 95% sample agreed with the results from the optical microscopy experiments. There are at least two lines observed for all temperatures below 25 °C. At 0 °C, there are four peaks observed corresponding to spacings of 38.9, 33.4, 32.0 and 29.2 Å possibly attributable to different phases. At 10 °C, there are two main peaks corresponding to *d* spacings of 33.7 and 30.8 Å. The cloudiness of the sample observed during optical microscopy experiments indeed supports the existence of multiple phases, but what are these phases? The 33.7 Å peak has a *d*/2 peak at 16.4 Å. This, coupled with the optical microscopy data, suggests that this is from a layer phase. The 30.8 Å peak is more difficult to define and could be attributed to solid, undissolved material in the sample. Unusually, a broad 87.5 Å peak appears at ~10 °C before disappearing above 30 °C. The 2-*d* images for the 95% mixture at 0 and 30 °C are displayed in Fig. 14 to further highlight this. It is unlikely that this broad peak is from the solid non-ionic since it is not present at 5 °C. One possible explanation is that the bilayers form a kind of mesh phase, but further experiments are required to establish this. On heating above 25 °C, the samples become one phase with *d* (33.7 Å) and *d*/2 (16.4 Å). On cooling to 0 °C, the sample again separates into two phases.

The diffraction patterns from similar measurements on the 90% sample also indicate the presence of a two-phase region at low temperatures (Fig. 15). Again, the small angle peaks observed at low temperatures could possibly be attributed to a bilayer phase with holes in it.

To check the structure of the suspected intermediate phase observed at low temperatures (below ~18.5 °C) for the 36% NaLAS/$C_{16}E_8$ mixture, a variable temperature scan was carried out (Fig. 16). The sample was heated every 10 °C between 0 and 70 °C after which only a diffuse ring attributable to a micellar solution could be seen. Below 20 °C, a different phase structure is clearly present. The fact that the two main peaks are close together indicates that this could possibly be an intermediate phase. On heating to 20 °C, one phase is present. It should be noted that the first and second order peaks observed do not correspond to *d* and $d/\sqrt{3}$ as predicted for a H_1 phase. However, this scan was carried out on a wide angle X-ray diffractometer and as such the small angle peaks are not very accurate. However, a difference in phase structure at low temperatures consistent with optical microscopy observations was confirmed.

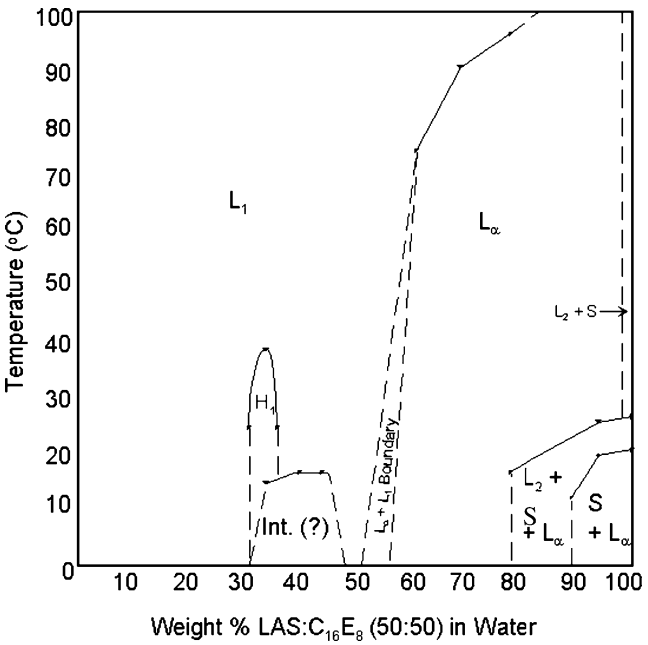

Fig. 17 Partial phase diagram for the NaLAS/$C_{16}E_8$/water system. *Solid lines* represent actual phase boundaries while broken line represent approximate phase boundaries

Differential scanning calorimetry

Differential scanning calorimetry measurements (0–110 °C) were carried out on selected samples of known composition (Table 7). These clearly show that no significant melting transitions occur at 80% surfactant or below. For 90–100% surfactant the data confirm the hysteresis reported above. Clearly, sample history needs to be considered in assessing the phase state of these samples.

Phase diagram and summary

The partial phase diagram for the NaLAS:$C_{16}E_8$/water system constructed using the data described above and is displayed in Fig. 17.

There are three major points for discussion in considering Fig. 17. What is the extent of mixing between the surfactants at low water concentrations? Why do the hexagonal and intermediate phases show such marked hysteresis? And the most important question, how useful are the packing constraint considerations in predicting the mesophase behaviour of mixed surfactants?

In considering the utility of the packing constraint considerations in predicting the mesophase behaviour of mixed surfactants, we can consider both the NaLAS:$C_{16}E_8$/water and the NaLAS:$C_{12}E_6$/water systems (Fig. 3). In both, we observe extensive regions of micellar solutions and lamellar phase, whilst the predicted phases are L_1, H_1, V_1 and L_α, followed by concentrated surfactant phases (solids, liquids etc.). This discrepancy is almost certainly because the head group area (a) values employed are inappropriate. The two surfactants have very different head groups. The hydrated NaLAS head group is compact and probably extends into the aqueous region by ca. 5 Å at the most. But the EO_8 can extend to ca. 33 Å, with an average coil-size of ca. 8 Å [C–C+C–O bond lengths × (no of bonds)$^{1/2}$]. Furthermore, because of its numerous different confirmations, it has a fairly open structure. For EO_6, the maximum extension and coil size are 25 Å and ca. 6 Å, respectively. Hence, the EO groups can occupy the space above the sulphonate groups, leading to a smaller area than expected. If this is taken into account, then the mesophase behaviour observed is in good agreement with packing constraint considerations. A further point to consider is that the mixed micelles will not all have an identical composition, thus their sizes will vary. Hence, the concentrations (volume fractions) at which mesophases form will be higher than those for pure surfactants. This is likely to be less important than the reduced head group areas described above.

The occurrence of the intermediate phase at lower temperatures than the V_1 cubic phase is somewhat remarkable because with non-ionic surfactants alone these phases always form at higher temperatures [13, 20]. However, with ionic surfactants, both cationic and anionic [19, 20], the opposite is true. Therefore, in the NaLAS:$C_{16}E_8$/water system, the LAS component dominates. Almost certainly, the structure formed is a type of mesh phase [18]. There is no simple description of why intermediate phases form rather than bi-continuous cubic phases.

Finally, concerning the phases formed at zero and low water concentrations, there is even less understanding. The non-ionic surfactant can be regarded as a weakly polar liquid, hence is not highly soluble in NaLAS. There are several different semi-solid phases present in neat NaLAS, which take days to reach an apparently stable state. Thus, considerable effort is required to fully identify the structures present. However, because of the importance for product formulation and manufacture, where "solid" NaLAS is often present together with numerous organic and inorganic materials, wise industrialists will be enthusiastic to fund this area.

Acknowledgment It is a pleasure to thank EPSRC and Unilever Research for financial support, together with CLRC Daresbury for the X-ray facilities.

References

1. Ockelford J, Narayan KS, Timimi BA, Tiddy GJT (2003) An upper critical point in a lamellar liquid crystalline phase. J Phys Chem 97:1487–1491
2. Richards C, Tiddy GJT, Casey S (2007) Lateral phase separation gives multiple lamellar phases in a "binary" surfactant/water system—the phase behaviour of sodium alkyl-benzene sulfonate/water mixtures. Langmuir 23:467–475
3. Ramaraju SM, Carroll BJ, Chambers JG, Tiddy GJT (2006) Colloids Surf A 288:77–85
4. Richards C, Tiddy GJT, Casey S (2006) Colloids Surf A 288:103–112
5. Clint JH (1992) Surfactant aggregation, ch 6. Blackie, Glasgow, pp 130–146
6. Israelachvili JN, Mitchell DJ, Ninham BW (1976) Theory of self-assembly of hydrocarbon amphiphiles into micelles and bilayers. J Chem Soc Faraday Trans II 72:1525–1568
7. Israelachvili JN (1985) Intermolecular and surface forces, 1st edn. Academic, London
8. Bostock T, Mitchell DJ, Tiddy GJT, Waring L, Mcdonald MP (1983) Phase-behavior of polyoxyethylene surfactants with water-mesophase structures and partial miscibility (cloud points). J Chem Soc Faraday Trans I 79:975–1000
9. Hassan S, Rowe W, Tiddy GJT (2001) Surfactant liquid crystals. In: Holmberg K (ed) Applied surface and colloid chemistry, vol 1. Wiley, Chichester, pp 465–508
10. Laughlin RG (1994) The aqueous phase behaviour of surfactants. Academic, London
11. Richards C, Casey S, Ramaraju SM, Carroll BJ, Chambers JG, Tiddy GJT (2007) In press
12. Corcoran J, Fuller S, Rahman A, Shinde N, Tiddy GJT, Attard G (1992) J Mater Chem 2(7):695–702
13. Funari SS, Holmes MC, Tiddy GJT (1994) Intermediate lyotropic liquid-crystal phases in the C16EO6/water system. J Phys Chem 98(11):3015–3023

14. Lide DR (1999) CRC handbook of chemistry and physics, 8th edn. CRC, Boca Ranton
15. Thompson L, Walsh JM, Tiddy GJT (1996) Colloids Surf A 106:223–235
16. Small DM (1986) The physical chemistry of lipids. Plenum, New York, Ch.2 pp 21–40 (Appendix 1, pp 561–563)
17. Lawrence A (1961) Surface activity and detergency. Macmillan, London
18. Funari SS, Holmes MC, Tiddy GJT (1992) Microscopy, X-ray diffraction and NMR studies of lyotropic liquid crystal phases in the $C_{22}EO_6$-water system—a new intermediate phase. J Phys Chem 96(26):11029–11038
19. Rendall K, Tiddy GJT, Trevethan MA (1983) Optical microscope and NMR studies of mesophases formed at compositions between hexagonal and lamellar phases in sodium *n*-alkanoate and water mixtures and related surfactant systems. J Chem Soc Faraday Trans 1(79):637
20. Blackmore ES, Tiddy GJT (1998) Phase behaviour and lyotropic liquid crystals in cationic surfactant-water systems. J Chem Soc Faraday Trans 2(84):1115–1127